Electronic structure, magnetic, and dielectric properties of the edge-sharing copper oxide chain compound NaCu₂O₂

Ph. Leininger, M. Rahlenbeck, M. Raichle, B. Bohnenbuck, A. Maljuk,* C. T. Lin, and B. Keimer

Max-Planck-Institut für Festkörperforschung, Heisenbergstr. 1, D-70569 Stuttgart, Germany

E. Weschke and E. Schierle

*Helmholtz-Zentrum Berlin für Materialien und Energie, Wilhelm-Conrad-Röntgen-Campus BESSY II,
Albert-Einstein-Straße 15, D-12489 Berlin, Germany*

S. Seki and Y. Tokura

Department of Applied Physics, University of Tokyo, Bunkyo-ku, Tokyo 113-8656, Japan

J. W. Freeland

Advanced Photon Source, Argonne National Laboratory, Argonne, Illinois 60439, USA
(Received 26 November 2009; published 17 February 2010)

We report an experimental study of NaCu₂O₂, a Mott insulator containing chains of edge-sharing CuO₄ plaquettes, by polarized x-ray absorption spectroscopy (XAS), resonant magnetic x-ray scattering (RMXS), magnetic susceptibility, and pyroelectric current measurements. The XAS data show that the valence holes reside exclusively on the Cu^{2+} sites within the copper-oxide spin chains and populate a d orbital polarized within the CuO₄ plaquettes. The RMXS measurements confirm the presence of incommensurate magnetic order below a Néel temperature of $T_N = 11.5$ K, which was previously inferred from neutron powder-diffraction and nuclear-magnetic-resonance data. In conjunction with the magnetic-susceptibility and XAS data, they also demonstrate an "orbital" selection rule for RMXS that is of general relevance for magnetic-structure determinations by this technique. Dielectric property measurements reveal the absence of significant ferroelectric polarization below T_N, which is in striking contrast to corresponding observations on the isostructural compound LiCu₂O₂. The results are discussed in the context of current theories of multiferroicity.

I. INTRODUCTION

Stimulated in part by the discovery of high-temperature superconductivity, copper oxides with spin-1/2 networks ranging from zero to three dimensions have been the focus of a large amount of research during the past two decades. Among these, Mott-insulating compounds that comprise spin chains with edge-sharing CuO₄ plaquettes have been of particular recent interest as models of frustrated magnetism in one dimension. In these materials, the Cu-O-Cu bond angle is close to 90° so that the magnitude of the superexchange coupling between nearest-neighbor Cu^{2+} spin-1/2 ions, J_1, is smaller than that of the next-nearest-neighbor coupling, J_2.[1] Depending on the sign and magnitude of the ratio J_1/J_2, as well as on the relative magnitudes of the spin-lattice coupling and the interchain exchange interactions, a variety of ground states have been observed in different members of this family, including spiral magnetism,[2–6] collinear antiferromagnetism,[7,8] and spin-Peierls order.[9] The quasi-one-dimensional spin correlations have been observed to profoundly affect charge excitations across the Mott-Hubbard gap.[10] In addition, charge order[11,12] and a spin-density-modulation[13] have been reported in materials with doped edge-sharing copper-oxide chains.

The recent discovery of ferroelectricity associated with helical magnetic order (multiferroicity) in the insulating edge-sharing copper-oxide chain compounds LiCu₂O₂ (Ref. 14) and LiCuVO₄ (Ref. 15) has stimulated another wave of research on this family of materials, and it has sparked a controversy about the origin of this effect. The magnetoelectric coupling is generally consistent with models according to which multiferroicity is an intrinsic consequence of spiral magnetism.[16–19] While some aspects of the experimental data on both compounds agree with specific predictions of these models,[14,20,21] disagreements with other predictions have also been pointed out.[14,19,22] An alternative explanation invokes orbital polarization of defects generated by intersubstitution of Li and Cu (whose ionic radii are closely similar) as the origin of the electric polarization.[23–25] This scenario is supported by the observation of substantial deviations from stoichiometry and substitutional disorder in both LiCu₂O₂ and LiCuVO₄.[4,26] However, the applicability of this model to LiCu₂O₂ has been disputed based on the results of a recent study on single crystals with nearly stoichiometric composition.[27,28]

We report the results of an experimental investigation of single crystals of NaCu₂O₂, a Mott insulator that is isostructural and isoelectronic to LiCu₂O₂ (Fig. 1). Like LiCu₂O₂ and LiCuVO₄,[2,4,6] NaCu₂O₂ exhibits helical magnetic long-range order at low temperatures due to competing ferromagnetic nearest-neighbor and antiferromagnetic next-nearest-neighbor superexchange interactions.[3,5,29] The main difference to the Li-based compounds is the large difference between the ionic radii of Na and Cu, which disfavors intersubstitution of both elements.[3,30] Experiments on NaCu₂O₂ thus offer the chance to elucidate the intrinsic properties of
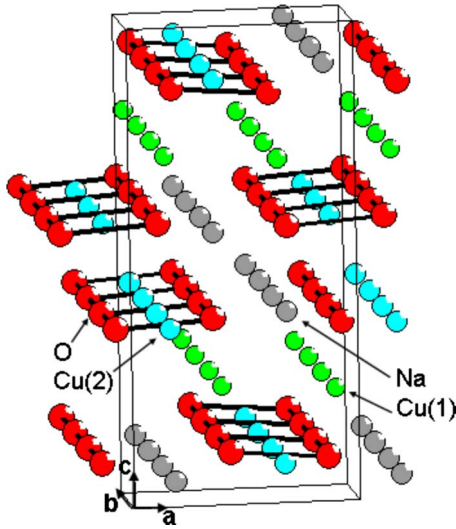
FIG. 1. (Color online) Sketch of the orthorhombic crystal structure of $NaCu_2O_2$ (space group *Pnma*). The room-temperature lattice parameters are $a=6.2087$ Å, $b=2.9343$ Å, and $c=13.0548$ Å (Ref. 30).

FIG. 2. (Color online) Polarization-dependent x-ray absorption spectra around the Cu L_3- and L_2-absorption edges of $NaCu_2O_2$. θ denotes the angle between the incident wave vector and the sample surface, which was parallel to the *ab* plane (see lower right inset). The origins of the peaks P_1, P_2, and P_3 are discussed in the text. The inset shows the θ dependence of the intensity of peak P_2 on an larger scale.

this class of compounds without interference from disorder.

This paper is organized as follows. Section II describes polarization-dependent XAS experiments designed to clarify the orbital character of the valence electrons in $NaCu_2O_2$. Section III contains the results of susceptibility and RMXS experiments aimed at elucidating the magnetic properties of $NaCu_2O_2$. Section IV summarizes measurements of the electrical polarization and the dielectric constant. In the concluding section, Sec. V, the results are contrasted with observations on $LiCu_2O_2$ and discussed in the light of current theories of multiferroicity.

II. ELECTRONIC STRUCTURE

We begin by describing XAS measurements near the Cu L-absorption edge aimed at determining the orbital character of the valence-electron states in $NaCu_2O_2$. The $NaCu_2O_2$ lattice structure contains copper ions in two nonequivalent sites [Cu(1) and Cu(2) in Fig. 1]. The chemical coordination and bond lengths of these ions indicate valence states of 1+ and 2+ (with electron configurations $3d^{10}$ and $3d^9$, and spins 0 and 1/2), respectively. However, a recent XAS study of the isostructural $LiCu_2O_2$ had come to the conclusion that the Cu(1) ions contain an intrinsic density of holes, independent of Li-Cu intersubstitution.[31] We have checked the validity of this conclusion on $NaCu_2O_2$, a compound in which the latter complication is manifestly absent.

The experiments were performed on an untwinned, plate-like single crystal with surface area 3×2 mm^2 and thickness 100 μm, which had been prepared by a self-flux technique already described elsewhere.[30] The sample surface is parallel to the *ab* plane of the orthorhombic crystal structure and hence includes the CuO_4 plaquettes (Fig. 1). The XAS data were taken at beamline 4-ID-C of the Advanced Photon Source in total-fluorescence-yield mode at a temperature of 150 K. The beam polarization was horizontal and the sample
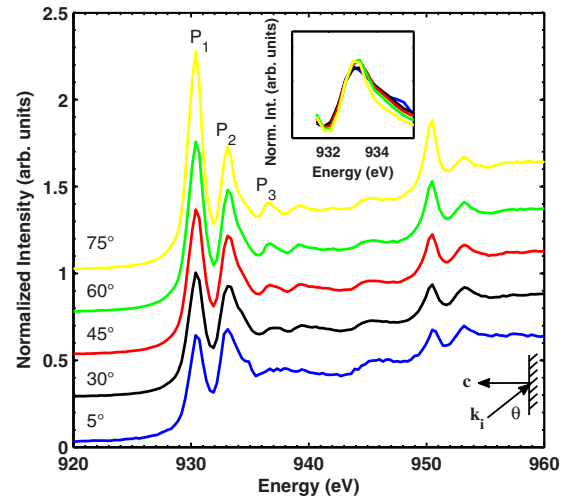
was rotated such that data could be taken with different angles, θ, between the incident wave vector $\mathbf{k_i}$ and the sample surface (Fig. 2). All spectra were normalized to the same intensity 10 eV above the Cu L_2-absorption edge.

Figure 2 shows a series of XAS spectra obtained for different θ. The features in the energy ranges 930–938 and 950–958 eV correspond to the Cu L_3- and L_2-absorption edges, respectively. At the L_3 edge, three peaks are observed. The energy splitting of 2.7 eV between the first peak (P_1) at 930.5 eV and the second peak (P_2) at 933.2 eV allows us to attribute P_1 to the Cu^{2+} ions on site Cu(2), and P_2 to the Cu^{1+} ions on site Cu(1).[31] The additional peak (P_3) at 936.7 eV is related to an excitation into nonlocal states.[32] When $\mathbf{k_i}$ is turned from in plane to out of plane, the intensity of P_1 is progressively enhanced, indicating that the valence hole on Cu^{2+} occupies d orbitals polarized within the CuO_4 plaquettes. The residual intensity observed for $\theta=5°$ can be related to the remaining in-plane orbital contribution. The same polarization dependence is observed at the Cu L_2-absorption edge. These findings agree with density-functional calculations for the structurally nearly identical $LiCu_2O_2$ compound, which predict that the states near the Fermi level are hybrids of the Cu $d_{x^2-y^2}$ orbital and O $p_{x,y}$ orbital in the CuO_2 chains.[19,33]

The intensity of peak P_2 originating from the Cu(1) ions is independent of θ within the experimental error (inset in Fig. 2), as expected for the spherically symmetric $2p^6 3d^{10}$ ground-state and $2p^5 3d^{10} 4s^1$ final-state configurations in the XAS excitation of Cu^{1+}. We note that our data are quite different from corresponding data on $LiCu_2O_2$ that revealed a strong polarization dependence of the P_2 peak intensity.[31] Based in part on electronic-structure calculations, the authors of Ref. 31 had attributed this observation to an intrinsic density of holes on the nominally monovalent copper ions, independent of the deviations from stoichiometry in $LiCu_2O_2$.
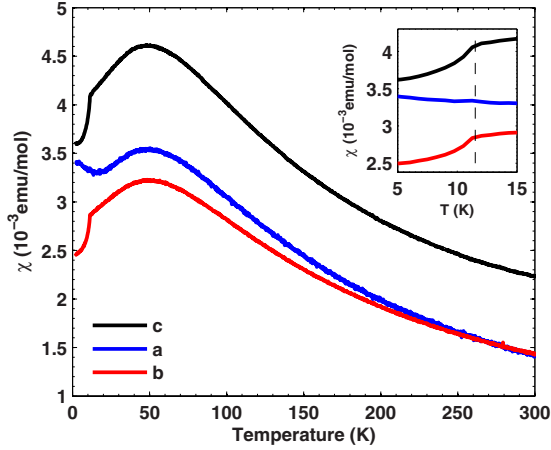
FIG. 3. (Color online) Temperature dependence of the magnetic susceptibility along the principal crystallographic axes measured with a magnetic field $H=1000$ Oe. The inset highlights the data at low temperature.

Our data on the stoichiometric but structurally nearly identical NaCu$_2$O$_2$ do not support this interpretation. Rather, they indicate that the Cu d orbitals on the Cu(1) sites of both compounds are fully occupied, as expected for the 1+ valence state, and that the polarization dependence of the corresponding XAS peak in LiCu$_2$O$_2$ originates from defects created by Li-Cu intersubstitution.

III. MAGNETIC PROPERTIES

Figure 3 shows the magnetic susceptibility, χ, measured on an untwinned crystal from the same batch as the one described above. The broad maximum around $T=50$ K is characteristic of short-range antiferromagnetic spin correlations in low-dimensional magnets. Upon cooling below the Néel temperature $T_N=11.5$ K, χ exhibits a sharp drop for magnetic fields, **H**, along b or c while a slight upturn is observed for **H**$\|a$. This implies that the direction of the magnetic moment in the Néel state is predominantly in the bc plane, consistent with a bc-polarized spiral inferred from neutron powder-diffraction and nuclear-magnetic-resonance (NMR) measurements.[3,5,34] A previously reported[3,5] anomaly in $\chi(T)$ for $T\sim8$ K was not observed in our samples. Measurements of $\chi(\mathbf{H})$ up to 7 T (not shown) did not reveal any anomalies indicative of spin-flop transitions.

RMXS measurements with photon energies near the Cu L_3 edge were performed in order to further investigate the spin correlations below T_N. The experiments were performed at the U46-PGM1 beamline at the BESSY II synchrotron in Berlin, Germany, using a two-circle diffractometer with horizontal scattering geometry designed at the Freie Universität Berlin. Silver paste was used to glue the crystal onto a copper goniometer attached to a continuous flow cryostat, such that the a and b axes were parallel to the diffraction plane. A 800-nm-thick aluminum foil provided sufficient heat shielding to reach sample temperatures as low as 3 K. The incident beam was polarized either horizontally (H) or vertically (V), i.e., parallel or perpendicular to the scattering plane. The
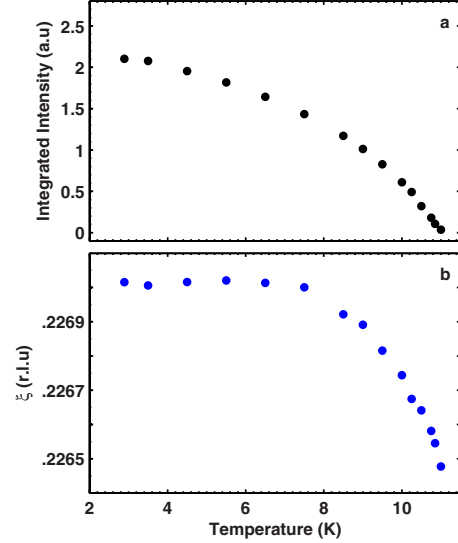

FIG. 4. (Color online) (a) Temperature dependence of the intensity of the magnetic Bragg reflection at $\mathbf{Q}=(0.5\ \xi\ 0)$, extracted from fits to RMXS data. (b) b-axis component of $\mathbf{Q}$ as a function of temperature.

diffracted beam was detected without polarization analysis.

At temperatures below T_N, a resonant diffraction peak was observed at wave-vector transfer $\mathbf{Q}=(0.5\ \xi\ 0)$, with incommensurate component $\xi\sim0.227$ along the spin chains. (The components of $\mathbf{Q}$ are indexed based on the orthorhombic crystal structure; see Fig. 1.) The origin of the peak was identified as magnetic based on the temperature dependence of its intensity [Fig. 4(a)]. The RMXS data thus confirm the propagation vector extracted from powder neutron-diffraction measurements.[3] The width of the diffraction peak, measured along the propagation vector, is temperature independent and yields a lower bound of 3500 Å on the magnetic domain size in the ab plane. The temperature variation in the incommensurate wave vector below T_N [Fig. 4(b)] is much smaller than the corresponding variation in LiCu$_2$O$_2$, where a two-step transition to magnetic long-range order was observed.[35,36] The energy dependence of the (0.5 ξ 0) peak intensity (Fig. 5) shows two minima at 931.6 and 934.3 eV, which can be attributed to strong absorption at the L_3 edges of Cu^{2+} and Cu$^+$ (dotted lines in Fig. 5). Similar data were reported for LiCu$_2$O$_2$ (Ref. 37). The resonant magnetic Bragg reflection was also observed when the photon energy was tuned to the Cu L_2-absorption edge of NaCu$_2$O$_2$ but an equivalent experiment at the Cu K edge yielded a null result. This is consistent with the expectation that the resonant enhancement of the RMXS cross section at transition-metal L edges is much larger than at K edges.

We now discuss the dependence of the RMXS cross section on the incident-beam polarization $\hat{\epsilon}_i$ and on the azimuthal angle Ψ. The scattering geometry and the definition of Ψ are illustrated in the inset of Fig. 6. Note that $\mathbf{Q}$ of the magnetic Bragg reflection approximately bisects the angle between the a and b axes, and that for $\Psi=0°$, the final wave vector $\mathbf{k}_f$ is nearly along $\hat{b}$ (and the outgoing polarization $\hat{\epsilon}_f$ hence nearly $\perp\hat{b}$). For $\Psi=180°$, on the other hand, $\mathbf{k}_f$ is nearly along $\hat{a}$ ($\hat{\epsilon}_f$ nearly $\perp\hat{a}$). According to the standard
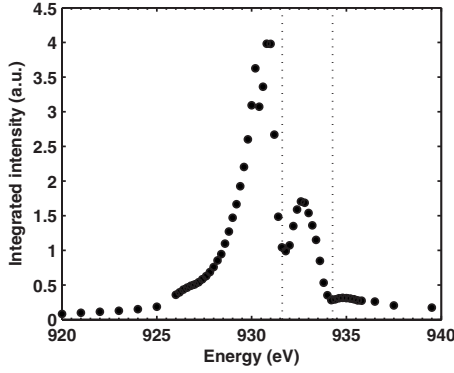
FIG. 5. Energy dependence of the scattered intensity at the (0.5 0.227 0) magnetic reflection near the Cu L_3-absorption edge. The data were taken at $T=3$ K. The dotted lines at 931.6 and 934.3 eV represent the energies of the Cu^{2+} and Cu^{1+} absorption edges, which were extracted from the widths of longitudinal momentum scans through the magnetic reflection.

treatment of RMXS,[38] the magnetic scattering amplitude is proportional to $(\hat{\epsilon}_f \times \hat{\epsilon}_i) \cdot \mathbf{m}$, where $\mathbf{m}$ is the magnetic moment. The susceptibility indicates that $\mathbf{m}$ is confined to the bc plane below T_N (Fig. 3). For $\Psi=0°$ and V (H) incident polarization, one would hence expect the scattering amplitude to be mainly proportional to $m_b(m_c)$ while for $\Psi=180°$, it should nearly vanish (be sensitive to both m_b and m_c). Since the susceptibility further indicates comparable magnitudes of m_b and m_c, the ratio I_V/I_H is expected to be of the order of unity for $\Psi=0°$ and to nearly vanish for $\Psi=180°$.

In striking contrast to this expectation, we have found that I_V is about three orders of magnitude smaller than I_H for $\Psi=0°$ [Fig. 6(a)]. Moreover, the azimuthal-angle dependence of the ratio I_V/I_H (which should not be strongly affected by distortions arising from sample size or surface effects) is well described by the function $A \sin^2 \Psi$ with $A \sim 1$ [Fig. 6(b)], which would imply $m_a \sim m_b \sim 0$ according to the standard description of RMXS.[38] A recent generalization of the theory of RMXS that takes the symmetry of the valence-electron wave function into account[39] resolves the apparent contradiction between the susceptibility and RMXS data. In the case at hand (which is explicitly treated in Ref. 39), it was shown that a selection rule precludes excitations of $2p$ core electrons into the partially occupied, planar $3d_{x^2-y^2}$ orbital of Cu^{2+} (see Sec. II) by vertically polarized photons. This implies that $I_V=0$ for both $\Psi=0°$ and $180°$. Our data thus confirm the revised analysis of Ref. 39 and highlight its importance for magnetic-structure determination by RMXS.

IV. DIELECTRIC PROPERTIES

Measurements of the electrical polarization $\mathbf{P}$ and the dielectric constant ε were performed on a $NaCu_2O_2$ crystal with dimensions $\approx 5 \times 2 \times 0.4$ mm^3. Due to the small thickness of the sample, the experiments were restricted to the c-axis components of both quantities. Electrodes were fabricated by covering the ab faces of the crystal by silver paste.

The sample was loaded into a 14 T cryomagnet and cooled down to 2 K while applying a poling electric field of
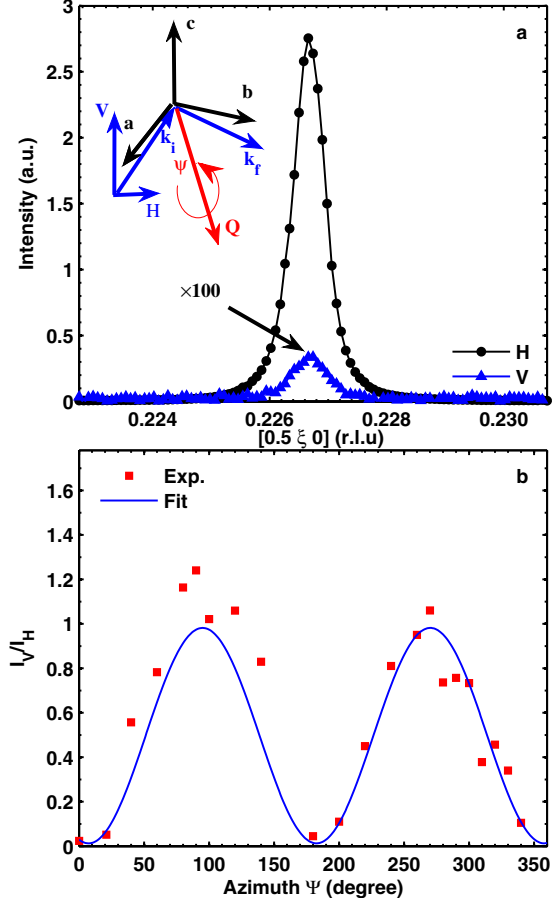

FIG. 6. (Color online) (a) Longitudinal reciprocal-space scans through the $\mathbf{Q}=(0.5\ \xi\ 0)$ reflection taken with horizontal (H) and vertical (V) polarization of the incident x-ray beam. The data for V polarization were multiplied by 100. (b) Azimuthal-angle (Ψ) dependence of the ratio of Bragg-peak intensities measured with V- and H-polarized incident beams. The line is the result of a fit to the function $A \sin^2 \Psi$, as discussed in the text. A small offset in Ψ was also included in the fit in order to account for imperfect sample alignment. The inset illustrates the definition of Ψ and the scattering geometry of $\Psi=0°$.

250 kV/m. Then, P_c was determined through a time integral of the pyroelectric current during a temperature sweep from 2 K with a rate of $+20$ K/min. ε_c was measured with an LCR meter operating at a frequency of 100 kHz with a temperature sweep rate of $+2$ K/min.

As shown in Fig. 7(a), neither a spontaneous nor a magnetic-field-induced electric polarization were detected for magnetic fields $\mathbf{H} \lesssim 14$ T within the experimental sensitivity of 0.3 $\mu C/m^2$. This upper bound is more than an order of magnitude lower than the P_c observed in $LiCu_2O_2$ for $T \ll T_N$.[14,20] The dielectric constant exhibits a subtle downturn upon cooling below T_N [Fig. 7(b)]. Effects of this magnitude have also been observed in other antiferromagnetic insulators[40] and may be a consequence of conventional spin-phonon coupling. Sharp spikes in the temperature dependence of ε_c such as the one observed at the Néel temperature of $LiCu_2O_2$ (Refs. 14 and 20) are not detected within the experimental sensitivity.
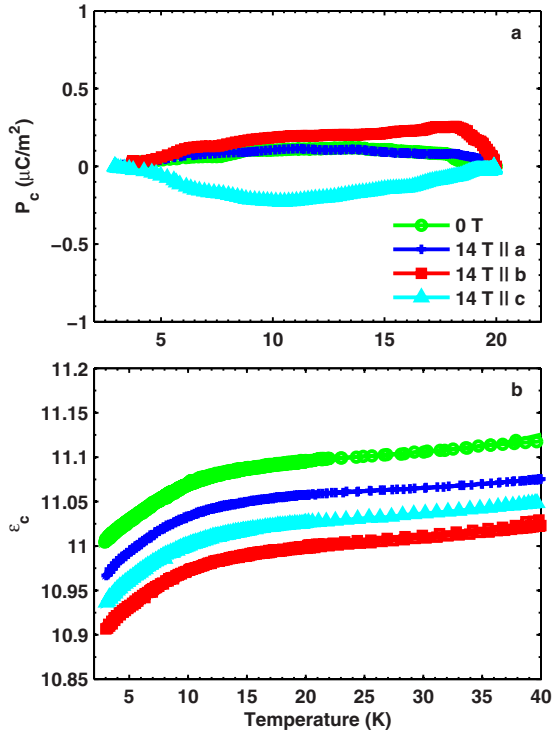
FIG. 7. (Color online) (a) Electrical polarization and (b) dielectric constant measured along the c axis for $\mathbf{H}=0$ and 14 T applied along the three principal crystallographic directions. The data in panel (b) were shifted vertically by arbitrary amounts $<5\%$ for clarity, and in order to take into account small changes in the electrode connections.

V. CONCLUSIONS

At first sight, the absence of multiferroicity in NaCu$_2$O$_2$ appears to contradict models that predict a ferroelectric polarization of the form $\mathbf{P} \propto \hat{n}_{ij} \times (\mathbf{S}_i \times \mathbf{S}_j)$ (where $\hat{n}_{ij}$ is a vector connecting nearest-neighbor spins $\mathbf{S}_{i,j}$) as an intrinsic consequence of spiral magnetism.[16–19] Neutron powder-diffraction and NMR measurements have indicated a bc-polarized spiral with propagation vector along b,[3,5] which is also consistent with the susceptibility and RMXS data presented here. The models thus predict a ferroelectric polarization along c, which was not observed (Fig. 7). Refinement of a compre-

hensive set of single-crystal magnetic neutron-diffraction data has, however, revealed a more complex magnetic structure in which the spin chains within the unit cell (Fig. 1) exhibit elliptical spiral states with opposite helicities[41] so that their ferroelectric polarizations (if present) are expected to cancel out. Our data are consistent with such an antiferroelectric state below T_N, and hence do not contradict the theoretical work of Refs. 16–18.

We have also shown that the Cu(1) sites of the NaCu$_2$O$_2$ structure exhibit a full-shell configuration and are hence electronically inactive. This agrees with prior considerations based on the chemical coordination of these sites but disagrees with the conclusions of a recent XAS study of LiCu$_2$O$_2$ according to which they exhibit an intrinsic density of holes.[31] The orbital polarization detected in the Cu(1) XAS spectra of LiCu$_2$O$_2$ is thus presumably a consequence of defects generated by Li-Cu intersubstitution. In view of the nearly identical lattice structures of LiCu$_2$O$_2$ and NaCu$_2$O$_2$, it seems natural to associate these defects with the ferroelectric polarization detected in LiCu$_2$O$_2$ but not in NaCu$_2$O$_2$. We cannot rule out, however, that the qualitative difference between the dielectric properties of both compounds originates in a subtle difference between their magnetic structures.

Finally, the simultaneous determination of the orbital occupation of the valence electrons of NaCu$_2$O$_2$ by XAS and their magnetic structure by RMXS allowed us to experimentally confirm an "orbital" selection rule for RMXS recently proposed on the basis of a theoretical analysis.[39] Especially for noncollinear spin structures, it is thus important to consider the orbital occupation before drawing conclusions about the spin polarization from RMXS data.

*Present address: Helmholtz-Zentrum Berlin für Materialien und Energie, D-14109 Berlin, Germany.

[1] Y. Mizuno, T. Tohyama, S. Maekawa, T. Osafune, N. Motoyama, H. Eisaki, and S. Uchida, Phys. Rev. B **57**, 5326 (1998).

[2] A. A. Gippius, E. N. Morozova, A. S. Moskvin, A. V. Zalessky, A. A. Bush, M. Baenitz, H. Rosner, and S.-L. Drechsler, Phys. Rev. B **70**, 020406(R) (2004).

[3] L. Capogna, M. Mayr, P. Horsch, M. Raichle, R. K. Kremer, M. Sofin, A. Maljuk, M. Jansen, and B. Keimer, Phys. Rev. B **71**, 140402(R) (2005).

[4] T. Masuda, A. Zheludev, B. Roessli, A. Bush, M. Markina, and

A. Vasiliev, Phys. Rev. B **72**, 014405 (2005).

[5] S.-L. Drechsler, J. Richter, A. A. Gippius, A. Vasiliev, A. A. Bush, A. S. Moskvin, J. Málek, Y. Prots, W. Schnelle, and H. Rosner, Europhys. Lett. **73**, 83 (2006).

[6] M. Enderle, C. Mukherjee, B. B. Fåk, R. K. Kremer, J.-M. Broto, H. Rosner, S.-L. Drechsler, J. Richter, J. Malek, A. Prokofiev, W. Assmus, S. Pujol, J.-L. Raggazzoni, H. Rakoto, M. Rheinstädter, and H. M. Rønnow, Europhys. Lett. **70**, 237 (2005).

[7] M. Boehm, S. Coad, B. Roessli, A. Zheludev, M. Zolliker, P. Boni, D. M. Paul, H. Eisaki, N. Motoyama, and S. Uchida, Eu-

rophys. Lett. **43**, 77 (1998).

[8] H. F. Fong, B. Keimer, J. W. Lynn, A. Hayashi, and R. J. Cava, Phys. Rev. B **59**, 6873 (1999).

[9] M. Hase, I. Terasaki, and K. Uchinokura, Phys. Rev. Lett. **70**, 3651 (1993).

[10] Y. Matiks, P. Horsch, R. K. Kremer, B. Keimer, and A. V. Boris, Phys. Rev. Lett. **103**, 187401 (2009).

[11] M. Matsuda, T. Yosihama, K. Kakurai, and G. Shirane, Phys. Rev. B **59**, 1060 (1999).

[12] P. Horsch, M. Sofin, M. Mayr, and M. Jansen, Phys. Rev. Lett. **94**, 076403 (2005).

[13] M. Raichle, M. Reehuis, G. Andre, L. Capogna, M. Sofin, M. Jansen, and B. Keimer, Phys. Rev. Lett. **101**, 047202 (2008).

[14] S. Park, Y. J. Choi, C. L. Zhang, and S.-W. Cheong, Phys. Rev. Lett. **98**, 057601 (2007).

[15] Y. Naito, K. Sato, Y. Yasui, Y. Kobayashi, Y. Kobayaashi, and M. Sato, J. Phys. Soc. Jpn. **76**, 023708 (2007).

[16] H. Katsura, N. Nagaosa, and A. V. Balatsky, Phys. Rev. Lett. **95**, 057205 (2005).

[17] I. A. Sergienko and E. Dagotto, Phys. Rev. B **73**, 094434 (2006).

[18] M. Mostovoy, Phys. Rev. Lett. **96**, 067601 (2006).

[19] H. J. Xiang and M.-H. Whangbo, Phys. Rev. Lett. **99**, 257203 (2007).

[20] S. Seki, Y. Yamasaki, M. Soda, M. Matsuura, K. Hirota, and Y. Tokura, Phys. Rev. Lett. **100**, 127201 (2008).

[21] F. Schrettle, S. Krohns, P. Lunkenheimer, J. Hemberger, N. Büttgen, H.-A. Krug von Nidda, A. V. Prokofiev, and A. Loidl, Phys. Rev. B **77**, 144101 (2008).

[22] Y. Yasui, Y. Naito, K. Sato, T. Moyoshi, M. Sato, and K. Kakurai, J. Phys. Soc. Jpn. **77**, 023712 (2008).

[23] A. Moskvin and S. Drechsler, Eur. Phys. J. B **71**, 331 (2009).

[24] A. S. Moskvin, Y. D. Panov, and S.-L. Drechsler, Phys. Rev. B **79**, 104112 (2009).

[25] A. S. Moskvin and S.-L. Drechsler, EPL **81**, 57004 (2008).

[26] A. V. Prokofiev, I. G. Vasilyeva, V. N. Ikorskii, V. V. Malakhov, I. P. Asanov, and W. Assmus, J. Solid State Chem. **177**, 3131 (2004).

[27] Y. Yasui, K. Sato, Y. Kobayashi, and M. Sato, J. Phys. Soc. Jpn. **78**, 084720 (2009).

[28] Y. Kobayashi, K. Sato, Y. Yasui, T. Moyoshi, M. Sato, and K. Kakurai, J. Phys. Soc. Jpn. **78**, 084721 (2009).

[29] M. Horvatic, C. Berthier, F. Tedoldi, A. Comment, M. Sofin, M. Jansen, and R. Stern, Prog. Theor. Phys. Suppl. **159**, 106 (2005).

[30] A. Maljuk, A. Kulakov, M. Sofin, L. Capogna, J. Strempfer, C. Lin, M. Jansen, and B. Keimer, J. Cryst. Growth **263**, 338 (2004).

[31] C. L. Chen, K. W. Yeh, D. J. Huang, F. C. Hsu, Y. C. Lee, S. W. Huang, G. Y. Guo, H.-J. Lin, S. M. Rao, and M. K. Wu, Phys. Rev. B **78**, 214105 (2008).

[32] M. A. van Veenendaal and G. A. Sawatzky, Phys. Rev. B **49**, 3473 (1994).

[33] Because of the nearly quadratic oxygen coordination of the Cu^{2+} ions (and in spite of the orthorhombic space-group symmetry), we use the term $d_{x^2-y^2}$ for an orbital with lobes pointing toward the oxygen ligands. This terminology is consistent with previous work.

[34] Note that in Fig. 1 of Ref. [3], the spiral was erroneously depicted as polarized in the *ab* plane. As stated correctly elsewhere in the article, a *bc*-polarized spiral actually yields the best refinement of the neutron powder-diffraction data.

[35] A. Rusydi, I. Mahns, S. Müller, M. Rübhausen, S. Park, Y. J. Choi, C. L. Zhang, S.-W. Cheong, S. Smadici, P. Abbamonte, M. v. Zimmermann, and G. A. Sawatzky, Appl. Phys. Lett. **92**, 262506 (2008).

[36] S. W. Huang, D. J. Huang, J. Okamoto, C. Y. Mou, W. B. Wu, K. W. Yeh, C. L. Chen, M. K. Wu, H. C. Hsu, F. C. Chou, and C. T. Chen, Phys. Rev. Lett. **101**, 077205 (2008).

[37] S. W. Huang, D. J. Huang, J. Okamoto, W. B. Wu, C. T. Chen, K. W. Yeh, C. L. Chen, M. K. Wu, H. C. Hsu, and F. C. Chou, Solid State Commun. **147**, 234 (2008).

[38] J. P. Hill and D. F. McMorrow, Acta Crystallogr. **52**, 236 (1995).

[39] M. Haverkort, N. Hollmann, I. Krug, and A. Tanaka, arXiv:0911.0705 (unpublished).

[40] T. Katsufuji and H. Takagi, Phys. Rev. B **64**, 054415 (2001).

[41] L. Capogna *et al.* (unpublished).